# Carboxyl group protonation upon reduction of the *Paracoccus denitrificans* cytochrome *c* oxidase: direct evidence by FTIR spectroscopy

Petra Hellwig[a], Borries Rost[a], Ulrike Kaiser[a], Christian Ostermeier[b], Hartmut Michel[b], Werner Mäntele[a,*]

[a] *Institut für Physikalische und Theoretische Chemie der Universität Erlangen-Nürnberg, Egerlandstrasse 3, 91058 Erlangen, Germany*
[b] *Max-Planck-Institut für Biophysik, Frankfurt, Germany*

Received 13 March 1996

**Abstract The redox reactions of the cytochrome *c* oxidase from *Paracoccus denitrificans* were investigated in a thin-layer cell designed for the combination of electrochemistry under anaerobic conditions with UV/VIS and IR spectroscopy. Quantitative and reversible electrochemical reactions were obtained at a surface-modified electrode for all cofactors as indicated by the optical signals in the 400–700 nm range. Fourier transform infrared (FTIR) difference spectra of reduction and oxidation (reduced-minus-oxidized and oxidized-minus-reduced, respectively) obtained in the 1800–1000 $cm^{-1}$ range reveal highly structured band features with major contributions in the amide I (1620–1680 $cm^{-1}$) and amide II (1580–1520 $cm^{-1}$) range which indicate structural rearrangements in the cofactor vicinity. However, the small amplitude of the IR difference signals indicates that these conformational changes are small and affect only individual peptide groups. In the spectral region above 1700 $cm^{-1}$, a positive peak in the reduced state (1733 $cm^{-1}$) and negative peak in the oxidized state (1745 $cm^{-1}$) are characteristic for the formation and decay of a COOH mode upon reduction. The most obvious interpretation of this difference signal is proton uptake by one Asp or Glu side chain carboxyl group in the reduced state and deprotonation of another Asp or Glu residue. Moreover, both residues could well be coupled as a donor-acceptor pair in the proton transfer chain. An alternative interpretation is in terms of a protonated carboxyl group which shifts to a different environment in the reduced state. The relevance of this first direct observation of protein protonation changes in the cytochrome *c* oxidase for vectorial proton transfer and the catalytic reaction is discussed.**

*Key words:* *Paracoccus denitrificans*; Cytochrome *c* oxidase; FTIR spectroscopy; Protein electrochemistry; Electron transfer; Proton transfer; Redox reaction

## 1. Introduction

Cytochrome *c* oxidase, the terminal enzyme of most respiratory chains, catalyses the reduction of dioxygen to water driven by the input of four electrons from soluble cytochrome *c*. In this process, four protons are taken up and consumed in water formation ('chemical protons'), and up to four protons are translocated across the membrane ('vectorial protons') to contribute to the formation of a proton gradient, which in turn drives an ATP synthase (for reviews on structural and functional properties of the cytochrome *c* oxidase, see [1-3]. Recently, structural information from X-ray crystallography on the complete *Paracoccus denitrificans* oxidase [4] and on the cofactors of beef-heart oxidase [5] has put discussions on the catalytic and proton transfer mechanism of this enzyme on new grounds. The previously proposed pathway of the electrons from the cytochrome *c* docking site to $Cu_A$ and via heme *a* to the binuclear site formed by $Cu_B$ and heme $a_3$ is now solidly established by the high-resolution X-ray structure [4], and two pathways for protons appear possible (for a detailed discussion, see [4]). One of them leads from two loops of subunit I via the side chains of Ser-291, Lys-354, Thr-351, the heme $a_3$ hydroxyl group, and the side chain of Tyr-280, to the catalytic site and could form the pathway of chemical protons. The other pathway, presumably for the vectorial protons, is less clearly defined through the enzyme, but includes a number of hydrogen-bonding (Asn-199, Asn-113, Asn-131) and ionizable side chains (Asp-124, Glu-278). Site-directed mutagenesis has pointed out the crucial role of some of these residues: replacement of Asn-113 or Asn-131 by hydrophobic amino acids blocks proton pumping, and replacement of Asp-124 by Asn also blocks proton pumping but not $O_2$ reduction. The redox midpoint potentials of the cofactors seem to depend on the pH, as demonstrated by equilibrium titrations and measurement of the heme reduction rates as a function of pH for the native and the $CN^-$ poisoned enzyme [6,7]. Although an overall proton uptake of 2.4 $H^+$ upon total reduction was observed for the beef heart mitochondrial enzyme [8], the sites of protonation are still unclear.

In order to understand the role of the protein in catalyzing dioxygen reduction and facilitating vectorial proton transfer, investigations of the enzyme in functionally relevant states with spectroscopic probes that monitor protein-specific properties, such as the microenvironment of the cofactors and the protonation states of amino acids potentially serving in a proton transfer chain, are necessary. Infrared (IR) spectroscopy can fill this gap, and provides a non-invasive probe for enzyme structure and function, with a sensitivity high enough to detect contributions of individual bonds to the spectrum (in particular when Fourier transform IR spectroscopy is used), and with time resolution to the nano- and picosecond domain which allows protein reactions to be followed in real time. The use of IR spectroscopy, with emphasis on reaction-induced difference techniques, is summarized in a recent review [9].

In the case of cytochrome *c* oxidase, steady-state and time-resolved IR spectroscopy has been extensively used to study

*Corresponding author. Fax: (49) (9131) 85-8307.
E-mail: MAENTELE@ATHENA.CHEMIE.UNI-ERLANGEN.DE

*Abbreviations:* IR, infrared; FTIR, Fourier transform infrared; SHE, standard hydrogen electrode; MOPS, 3-[*N*-morpholino]propanesulfonic acid.


*PII* S0014-5793(96)00342-0

the binding and dynamics of ligands (CO, $CN^-$, $N_3^-$) bound to the metal centers (for a recent review, see [10]). In these studies, the strong stretching modes of the ligands, all located in a 'window region' around 1970 $cm^{-1}$ (CO), 2050–2150 $cm^{-1}$ ($CN^-$), or 2000–2050 $cm^{-1}$ ($N_3^-$), were either analyzed straightforward in absorbance spectra or by following the photochemical dissociation and the rebinding of the ligand in steady-state or time-resolved difference spectra. In the absence of these ligands, which present elegant and easily accessible probes but also perturb the binding site as compared to the native or oxygenated enzyme, IR investigations are restricted to the analysis of the major protein absorbance bands. In such IR studies aimed at questions on the structure and stability of the oxidase, the amide I band profile was analyzed for the secondary structure and thermal stability of the enzyme [11-13].

In previous work, we introduced the combination of protein electrochemistry and FTIR difference spectroscopy as a technique for the study of redox proteins and redox-sensitive enzymes. Redox transitions of a protein-bound cofactor, initiated by electron transfer to or from a transparent electrode in a thin-layer spectroelectrochemical cell, lead to FTIR difference spectra as sensitive for individual bonds of the protein (and the cofactor) as are light-induced difference spectra. Moreover, individual cofactors can be addressed by selecting the appropriate electrode potential ('...dial a cofactor'), and vibrational difference spectra can thus be redox titrated. The redox-induced FTIR difference spectra, typically recorded for the 1800–1000 $cm^{-1}$ range, contain the full information on the reorganization of the cofactor and its protein site upon electron transfer, including local and global protein conformational changes, or protonation of side chain groups which could be the clue to the mechanism of redox-driven proton transfer. The technical aspects of this 'FTIR spectroelectrochemistry' and its application for the study of cofactor-protein interactions and protein reactions in electron transfer of the bacterial photosynthetic reaction center, of heme proteins and of a copper protein have been described [14-20].

Recently, Dodson et al. [21] elegantly applied these techniques for the study of CO binding to cytochrome *c* oxidase, analyzing the strong CO mode around 1960 $cm^{-1}$ as a function of the redox state of the cofactors. The pathlength of their electrochemical cell, however, limited this study to the analysis of ligand binding to the active site of the enzyme. Direct information on the protein could not be obtained, since the mid-infrared range from 1800 to 1000 $cm^{-1}$, which contains most of the diagnostically relevant modes, was not accessible. In the work presented here, we have used protein electrochemistry in an ultra-thin-layer electrochemical cell in the absence of a ligand to obtain access to protein vibrational modes in this region and to examine protein function in the physiologically relevant states.

## 2. Materials and methods

### 2.1. Sample preparation

Cytochrome *c* oxidase from *P. denitrificans* was prepared as reported for the crystallization procedure [22], but lacking the antibody fragment. For FTIR investigations, cytochrome *c* oxidase solubilized in dodecylmaltoside in 200 mM phosphate buffer (pH 6.9) was concentrated to approx. 0.5 mM using Microcon ultrafiltration cells. Exchange of $^1H_2O$ against $^2H_2O$ was performed by repeatedly concentrating the enzyme and rediluting in a $^2H_2O$ buffer. $^1H/^2H$ exchange was found to be better than 80% as judged from the shift of the amide II mode.

### 2.2. Electrochemistry

The ultra-thin spectroelectrochemical cell for the UV/VIS and IR range used here was previously described [14,15,23]. Sufficient transmission in the entire 1800–1000 $cm^{-1}$ range, even in the region of strong water absorbance at 1650 $cm^{-1}$, was achieved with the cell pathlength set to 6–8 μm. The gold grid working electrode was chemically modified according to a procedure described in [14] by adding a 1 mM solution of 4,4'-dithiodipyridine solution. In order to accelerate the redox reaction, mediators were added as previously described [23] to a final total concentration of 40 μM. At this concentration, and with the pathlength below 10 μm, no spectral contributions from the mediators in the VIS and IR range could be detected in control experiments with samples lacking the protein. As a supporting electrolyte, 100 mM KCl was added. Approx. 5–6 μl of the protein solution were sufficient to fill the spectroelectrochemical cell. Potentials quoted with the data refer to the Ag/AgCl/3 M KCl reference electrode unless otherwise specified; add +208 mV for SHE potentials.

### 2.3. Spectroscopy

FTIR and UV/VIS difference spectra as a function of the applied potential were obtained simultaneously from the same sample with a setup combining an IR beam from the interferometer for the 4000–1000 $cm^{-1}$ range and a dispersive spectrometer for the 400–1000 nm range as previously described [9,15]. First, the protein was equilibrated with an initial potential at the electrode, and single-beam spectra in the VIS and IR range were recorded. A potential step to the final potential was then applied, and single-beam spectra of this state were again recorded after equilibration. Difference spectra as presented here were then calculated from the two single-beam spectra with the initial single-beam spectrum taken as reference. No smoothing, baseline correction, or deconvolution procedures were applied. The equilibration process for each applied potential was followed by monitoring the electrode current and by successively recording spectra in the visible range until no further changes were observed, and generally took less than 10 min under the conditions (electrode modification, mediators) reported. Typically, 128 interferograms at 4 $cm^{-1}$ resolution were co-added for each single-beam IR spectrum and transformed using triangular apodization.

## 3. Results and discussion

Fig. 1 shows the reduced-minus-oxidized FTIR difference spectrum (full line) of *P. denitrificans* cytochrome *c* oxidase for a potential step from +0.5 to −0.2 V. For this potential step, a transition from the fully oxidized state of the cofactors to the fully reduced state should be observed. Difference bands corresponding to the reduced state point upward, and those that correspond to the oxidized state point downward. The FTIR difference spectrum for the reverse process, i.e. for a potential step from −0.2 to +0.5 V (dashed-dotted line) represents the exact mirror image, indicating quantitative and fully reversible electrochemical reactions at the electrode. Even minor bands such as the band structures between 1800 and 1680 $cm^{-1}$ or those between 1500 and 1200 $cm^{-1}$ are perfectly reversible. In view of the widespread use of resolution enhancement, data smoothing, baseline correction, deconvolution procedures and interactive (i.e. arbitrarily scaled) blank subtractions in FTIR spectroscopy of proteins, it should be noted again that none of these procedures were applied for the spectra shown here. The inset of Fig. 1 shows the corresponding difference spectra for the 400–700 nm range, with signals at 605 nm (heme *a*, heme $a_3$), 480 nm ($Cu_A$), and at 445 and 418 nm. For the comparison of spectra from different samples, which might differ in concentration

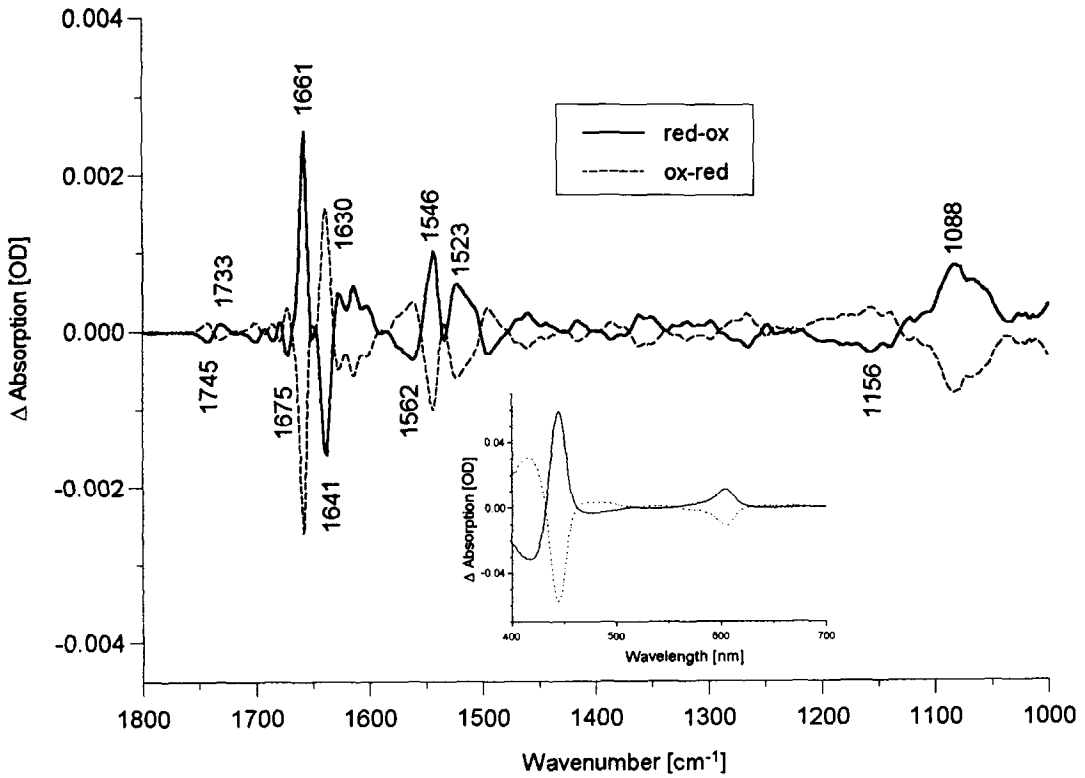


Fig. 1. Reduced-minus-oxidized (red-ox, full line) FTIR difference spectrum of cytochrome *c* oxidase obtained for a potential step from +0.5 to −0.2 V (vs. Ag/AgCl/3 M KCl). The dashed-dotted line corresponds to the reverse difference spectrum obtained for a potential step from −0.2 to +0.5 V. Conditions: approx. 0.5 mM cytochrome *c* oxidase in 200 mM phosphate buffer pH 6.9 with 100 mM KCl as electrolyte and mediators at a total concentration of 40 μM (composition see section 2). 128 interferograms were co-added for each single-beam spectrum; spectral resolution was 4 $cm^{-1}$. Inset: difference spectrum obtained from the same sample in the visible spectral range.

and in the pathlength of the electrochemical cell, these signals in the visible range serve for normalization.

The amplitudes of the FTIR difference signals are small, reaching at most $4\times10^{-3}$ for the strongest difference signal, a positive band at 1661 $cm^{-1}$ indicative of the reduced state. The prominent band in the IR absorbance spectrum (data not shown) is the amide I mode peaking at approx. 1658 $cm^{-1}$, which represents mainly the peptide C=O mode. Relating the total absorbance of the protein at this peak, which is between 0.4 and 0.6 in these samples, to the amplitude of the strongest difference signals (Fig. 1), we must conclude that the redox process affects only a small number of peptide groups, and that the major part of the protein acts as an inert scaffold. In the difference spectrum, four spectral regions, 1680–1620, 1560–1520, 1200–1000 and 1700–1750 $cm^{-1}$, with characteristic difference signals can be distinguished. For the discussion of the band structures in these ranges, we refer to the reduced-minus-oxidized difference spectrum (full line in Fig. 1), with the peak frequencies labeled.

In the 1680–1620 $cm^{-1}$ range, a sharp difference peak with a positve band at 1661 $cm^{-1}$ and a negative signal at 1641 $cm^{-1}$, but also the positive difference signal at 1630 $cm^{-1}$ all are clearly within the range of the amide I (predominantly a peptide C=O mode) absorbance of the polypeptide backbone. There is no evidence for further amide I components or for heterogeneous difference signals. Echabe et al. [13] have analyzed the amide I frequency range for a determination of secondary structure components. Their decomposition yielded a component at 1658 $cm^{-1}$ which gave 50% of the entire band area and was assigned to α-helical structures, but also smaller components with significant contributions at 1643 and 1630 $cm^{-1}$ as well as some small components at high frequencies (above 1680 $cm^{-1}$). At the present state of our work, we tend to assign the difference signals in the amide I range to alterations of these secondary structure elements upon the redox reaction, keeping in mind that only a few amide modes seem to be affected and thus no global rearrangements of the protein can be anticipated. A possible scenario for these alterations is the response of peptide dipoles to an altered electrostatic field originating from the cofactor(s) in their altered redox state. Responses in dipole strength, which would result in hypochromism or hyperchromism depending on the orientation, or in dipole direction, are also conceivable. However, we cannot exclude contributions from amino acid side chains in this region. At the upper end of this spectral range, smaller difference signals are observed between 1680 and 1700 $cm^{-1}$, in particular a peak at approx. 1682 $cm^{-1}$ in the reduced state. In this region, the heme propionates are expected to contribute, and a positive signal could indeed indicate protonation of a heme propionate upon reduction of the enzyme.

In the spectral region from 1560 to 1520 $cm^{-1}$, contributions from the amide II mode of the polypeptide, which is a coupled NH bending and CN stretching mode, can be expected. The 1546 $cm^{-1}$ signal is well within the typical range, and could be expected to be an alteration of the amide II mode coupled to (one of the) alterations of the amide I modes discussed above. However, a number of strong modes from aromatic amino acid side chain groups may also contribute in

this range, and an amide II assignment is less probable, in particular since the 1546 and 1523 $cm^{-1}$ bands did not exhibit a significant shift in preliminary investigations of the reduced-minus-oxidized difference spectrum in $^2H_2O$ (data not shown).

Echabe at al. [13] have assigned a characteristic absorbance band at 1515 $cm^{-1}$ (in $^2H_2O$) to the tyrosine C-C ring stretching mode. Alterations at specific tyrosine residues could, for example, account for the difference signal at 1523 $cm^{-1}$, but would have to await investigations of site-directed mutants for a definitive assignment.

A broad difference structure with a negative lobe at 1156 $cm^{-1}$ and a positive lobe at 1088 $cm^{-1}$ with a low-frequency shoulder is observed in the third spectral region under consideration. In the present investigations, phosphate buffer (200 mM) at pH 6.9 was used. If other buffers like Tris, HEPES or MOPS are used in this pH range (data not shown), these difference signals are absent and difference signals in other spectral regions characteristic for the respective buffers are present. We thus attribute the difference structures at 1156 and 1088 $cm^{-1}$ unequivocally to the PO modes from the phosphate buffer. Model IR absorbance spectra of phosphate buffers show strong PO modes at approximately the same frequencies, and difference spectra with exactly the same band structures between 1200 and 1000 $cm^{-1}$ as those in Fig. 1 can be calculated from two IR spectra of phosphate buffers at different pH. The sign of the difference bands in the reduced-minus-oxidized difference spectrum (solid line in Fig. 1) is indicative of deprotonation of phosphate groups, and is in line with the proton uptake by the oxidase. IR difference spectra, provided that suitable buffer modes are present, can thus be used for the detection of proton uptake or release by an enzyme, as previously shown for a bacterial cytochrome $bc_1$ complex [24]. At present, we attempt to calibrate the buffer difference spectra to allow a more precise determination of proton uptake ($H^+/e^-$) stoichiometries.

The most fascinating spectral region is certainly the 1680–1750 $cm^{-1}$ range which includes the COOH modes of protonated Asp and Glu side chains. In this range, two difference signals, a positive band at 1733 $cm^{-1}$ and a negative band at 1745 $cm^{-1}$, are observed for the reduced-minus-oxidized spectrum (Fig. 1). These difference signals are fully reversible upon oxidation as indicated by the dashed-dotted line. For the discussion of these signals, the spectral region from 1710 to 1770 $cm^{-1}$ is shown enlarged in Fig. 2. Both signals at 1733 $cm^{-1}$ (reduced state) and at 1745 $cm^{-1}$ (oxidized state) exhibit approximately equal strength, with peak amplitudes in the order of $2–3 \times 10^{-4}$ absorbance units. Based on the sample concentration which can be determined from the difference spectra in the visible range (Fig. 1, inset), the extinction coefficients of the vibrational modes which might be assigned to these difference signals are in the order of 200–400 l $mol^{-1}$ $cm^{-1}$ and thus match well those of Asp or Glu side chain modes (for IR extinction coefficients of amino acid side chain modes, see [25]). It is thus tempting to attribute these difference signals to the COOH side chain modes of individual Asp or Glu residues. This attribution is further strengthened by the downshift of both peaks by approx. 4 $cm^{-1}$ upon $^1H_2O/^2H_2O$ exchange (see dashed-dotted line in Fig. 2). The oxidase samples in $^2H_2O$ differed in concentration from that in $^1H_2O$; the difference signal was thus normalized on the concentration of the $^1H_2O$ sample on the basis of the difference spectra in the visible spectral range. A shift of several wavenumbers (around 10 $cm^{-1}$) is observed upon $^1H/^2H$ exchange for the protonated side chains of Asp and Glu residues in model compounds [25], and was previously observed to be 4–10 $cm^{-1}$ for other proteins [26,27]. We take the spectral region and the observed shift as a conclusive argument to definitely attribute the signals to Asp or Glu COOH modes in the reduced (1733 $cm^{-1}$) and the oxidized (1745 $cm^{-1}$) state of the enzyme.

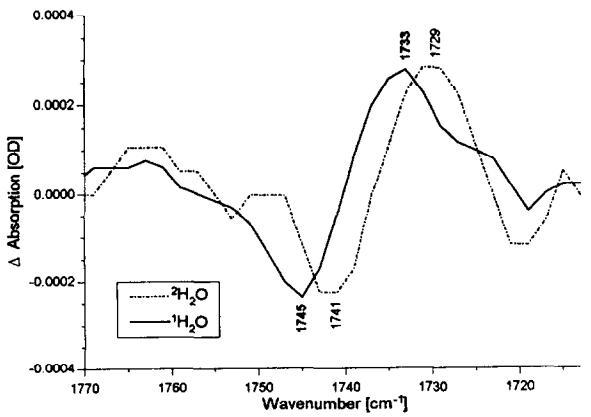


Fig. 2. Expanded view of the reduced-minus-oxidized difference spectrum from Fig. 1. Full line: sample equilibrated in $^1H_2O$; dashed-dotted line: sample equilibrated in $^2H_2O$.

In order to explain the shape of these difference signals with almost equal positive and negative components, the following scenarios are conceivable: (i) The protonation/deprotonation processes upon reduction of the enzyme can be understood as occurring independently at different residues, i.e. as deprotonation of one residue $R_1$ (protonated in the oxidized form) and protonation of another residue $R_2$ (deprotonated in the oxidized form):

oxidized enzyme ⇒ reduced enzyme

$$R_1-COOH \Rightarrow R_1-COO^- + H^+$$

$$R_2-COO^- + H^+ \Rightarrow R_2-COOH$$

(ii) Both processes could well be coupled mechanistically as a proton transfer from residue $R_1$ to residue $R_2$, and might represent a possibility for proton transfer within the enzyme:

oxidized enzyme ⇒ reduced enzyme

$$R_1-COOH + R_2-COO^- \Rightarrow R_1-COO^- + R_2-COOH$$

At the present stage, both scenarios are equally probable and would both account for the signal shape observed, and further experiments using site-directed mutants will be needed to distinguish between them. A third, although less likely possibility is that a residue $R_3$ is protonated in both the oxidized and the reduced state of the enzyme, but experiences a change of environment upon reduction. Both the amplitude of the signal and the sensitivity to $^1H_2O/^2H_2O$ exchange seem to favour the interplay between two Asp/Glu residues, however, the third possibility cannot be ruled out definitely.

If protonation/deprotonation reactions at residues $R_1$ and $R_2$ or a coupled proton transfer reaction are assumed, the

peak frequencies of the signals and the shift upon $^1H_2O/^2H_2O$ exchange allow one to speculate on the nature of the residues involved. Both residues must be fully accessible to protons and can exchange completely in $^2H_2O$, since the entire band feature is shifted. This is supported by the peak frequencies for the negative and the positive signal, which are rather indicative for groups able to form hydrogen bonds than for groups embedded in a non-protic environment. Along these lines, the scenario of a proton transfer from $R_1$ to $R_2$ would imply transfer from a less H-bonded COOH group (1745 $cm^{-1}$) to a more H-bonded COOH group (1733 $cm^{-1}$). This would contradict transfer to the inside of the protein; however, correlation of the 'global' environment with COOH frequencies is not that clear-cut and other factors such as bound water molecules could influence the frequency of a COOH mode much more.

Vectorial transfer of a proton might be achieved by a redox-induced p*K* shift leading to protonation/deprotonation reactions. The normalized signals in $^2H_2O$ have approximately the same amplitude as the signals in $^1H_2O$; there is apparently no influence on the p*K*. On the other hand, observation of protonation of an Asp or Glu residue at neutral pH implies that the p*K* of the respective group is considerably higher than for an isolated Asp or Glu in an aqueous environment. Redox-induced shifts of the p*K* should thus be from much higher than 7 to a value considerably lower in order to allow proton uptake/release.

At the present stage, it is still too early to speculate on the groups involved in this protonation/deprotonation or proton transfer reaction, and detailed investigations on the pH dependence of the difference signals as well as of mutants will be necessary for a conclusive assignment to specific Asp or Glu residues. However, the X-ray structure [4] suggests some key residues which could be involved in vectorial or chemical proton transfer (such as Asp-399, Glu-278, and Asp-124). These residues are probable candidates for the FTIR difference signals at 1745 $cm^{-1}$/1733 $cm^{-1}$.

## 4. Conclusions

The FTIR difference signal at 1745 $cm^{-1}$/1733 $cm^{-1}$ represents the first direct spectroscopic evidence for protonation/deprotonation reactions at amino acid side chain groups in cytochrome *c* oxidase, and opens new access to the investigation of the catalytic mechanism and the mechanism of vectorial proton transfer for this enzyme. Infrared spectroscopy has been extremely useful for the study of ligand binding and dynamics, but it is evident that the combination of protein electrochemistry and FTIR spectroscopy enlarges the horizon to detailed studies of the reactions of the protein. It is still too early to speculate on an assignment of the FTIR difference signals to specific amino acids, and extensive investigations of the pH dependence of the signals and of mutants will be necessary. However, it is clear that the FTIR difference spectra shown here contain abundant information on the reorganization of the protein upon electron transfer, and start to be the key for the understanding of the relation between the structure and the function of the enzyme.

*Acknowledgements:* The authors would like to thank S. Grzybek and E. Hamacher (Universität Erlangen) for valuable discussions and critical reading of the manuscript, and Prof. B. Ludwig for supplying *Paracoccus* membranes as well as for valuable discussions.

## References

[1] Saraste, M. (1990) Q. Rev. Biophys. 23, 331–366.
[2] Babcock, G.T. and Wikström, M. (1992) Nature 356, 301–309.
[3] Calhaun, M.W., Thomas, J.W. and Gennis, R.B. (1994) Trends Biochem. Sci. 19, 325–330.
[4] Iwata, S., Ostermeier, C., Ludwig, B. and Michel, H. (1995) Nature 376, 660–669.
[5] Tsukihara, T., Aoyama, H., Yamashita, E., Tomizaki, T., Yamaguchi, H., Shinzawa-Itoh, K., Nakashima, R., Yaono, R. and Yoshikawa, S. (1995) Science 269, 1069–1074.
[6] Moody, A.J. and Rich, P.R. (1990) Biochim. Biophys Acta 1015, 205–215.
[7] Verkhovsky, M.I., Morgan, J.E. and Wikström, M. (1995) Biochemistry 34, 7483–7491.
[8] Mitchell, R. and Rich, P.R. (1994) Biochim. Biophys. Acta 1186, 19–26.
[9] Mäntele, W. (1993) Trends Biochem. Sci. 18, 197–202.
[10] Caughey, W.S., Dong, A., Sampath, V., Yoshikawa, S. and Zhao, X.-J. (1993) J. Bioenerg. Biomembr. 25, 81–91.
[11] Haltia, T., Semo, N., Arrrondo, J.L.R., Goñi, F.M. and Freire, E. (1994) Biochemistry 33, 9731–9740.
[12] Arrondo, J.L.R., Castresana, J., Valpuesta, J.M. and Goñi, F.M. (1994) Biochemistry 33, 11650–11655.
[13] Echabe, I., Haltia, T., Freire, E., Goñi, F.M. and Arrondo, J.L.R. (1995) Biochemistry 34, 13565–13569.
[14] Moss, D.A., Nabedryk, E., Breton, J. and Mäntele, W. (1990) Eur. J. Biochem. 187, 565–572.
[15] Mäntele, W. (1996) in: Biophysical Techniques in Photosynthesis (Hoff, A.J. and Amesz, J. eds.) Chapter 9, pp. 137–160, Kluwer, Dordrecht in press.
[16] Schlereth, D.D. and Mäntele, W. (1992) Biochemistry 31, 7494–7502.
[17] Schlereth, D.D. and Mäntele, W. (1993) Biochemistry 33, 1118–1126.
[18] Leonhard, M. and Mäntele, W. (1993) Biochemistry 32, 4532–4538.
[19] Bauscher, M., Leonhard, M., Moss, D.A. and Mäntele, W. (1993) Biochim. Biophys. Acta 1183, 59–71.
[20] Brischwein, M., Scharf, B., Engelhard, M. and Mäntele, W. (1993) Biochemistry 32, 13710–13717.
[21] Dodson, E.D., Zhao, X.-J., Caughey, W.S. and Elliot, C.M. (1996) Biochemistry 35, 444–452.
[22] Ostermeier, C., Iwata, S., Ludwig, B. and Michel, H. (1995) Nat. Struct. Biol. 2, 842–846.
[23] Baymann, F., Moss, D.A. and Mäntele, W. (1991) Anal. Biochem. 199, 269–274.
[24] Baymann, F. (1995) PhD Thesis, Fakultät für Biologie, Universität Freiburg, Germany.
[25] Venyaminov, S.Y. and Kalnin, N.N. (1990) Biopolymers 30, 1243–1257.
[26] Siebert, F., Mäntele, W., and Kreutz, W. (1982) FEBS Lett. 141, 82–87.
[27] Hienerwadel, R., Grzybek, S., Fogel, C., Kreutz, W., Okamura, M.Y., Paddock, M.L., Breton, J., Nabedryk, E. and Mäntele, W. (1995) Biochemistry 34, 2832–2843.